

Utilizing force paddles for mean propulsive force measurements in swimming

A study on force paddle reliability and the possibility to measure propulsive forces and power outputs in swimming

Degree project report in Applied Mechanics

ANTON WALLIN

DEPARTMENT OF INDUSTRIAL AND MATERIALS SCIENCE

CHALMERS UNIVERSITY OF TECHNOLOGY
Gothenburg, Sweden 2024
www.chalmers.se

DEGREE PROJECT REPORT 2024

Utilizing force paddles for mean propulsive force measurements in swimming

A study on force paddle reliability and the possibility to measure propulsive forces and power outputs in swimming

ANTON WALLIN



CHALMERS
UNIVERSITY OF TECHNOLOGY

Department of Industrial and Materials Science
CHALMERS UNIVERSITY OF TECHNOLOGY
Gothenburg, Sweden 2024

Utilizing force paddles for mean propulsive force measurements in swimming
A study on force paddle reliability and the possibility to measure propulsive forces
and power outputs in swimming
ANTON WALLIN

© ANTON WALLIN, 2024.

Supervisor: Martin Fagerström, Department of Industrial and Materials Science
Examiner: Martin Fagerström, Department of Industrial and Materials Science

Degree project report 2024
Department of Industrial and Materials Science
Chalmers University of Technology
SE-412 96 Gothenburg
Sweden
Telephone +46 31 772 1000

Cover: An example of propulsive pressures measured by **eo** SwimBETTER handsets
in freestyle swimming.

Typeset in L^AT_EX
Gothenburg, Sweden 2024

Utilizing force paddles for mean propulsive force measurements in swimming
A study on force paddle reliability and the possibility to measure propulsive forces
and power outputs in swimming

ANTON WALLIN

Department of Industrial and Materials Science
Chalmers University of Technology

Abstract

Right now, there is a rapid development within swimming where large number of data points are used to quantify and improve the swimming performance [1]. One of the sensors that is used to gather this performance data is the **eo** SwimBETTER force paddles that measures the propulsive pressure on the palms of a swimmers hands with sensor filled handsets [2].

In this report, I present the results from a project where I have studied if it could be possible to use the **eo** SwimBETTER handsets to measure the power output of a swimmer. The first part of the project was focused on studying the reliability of the **eo** SwimBETTER measurements where I focused on the repeatability of the **eo** SwimBETTER handsets and the pressure sensor accuracy. In the second part of the project, I performed an initial study of the possibility to use the **eo** SwimBETTER handsets to measure the mean propulsive force of a swimmer. I tried to design a method for converting the propulsive pressure measured by the **eo** SwimBETTER handsets into a mean propulsive force. Measuring the mean propulsive force of a swimmer could then be an integral part in a method for measuring the power output of a swimmer.

For the reliability part, it was found that the repeatability appears to be good regarding the mean propulsive pressure. The method used has some limitations regarding the repeatability of the instantaneous propulsive pressure but more resources would probably be required to get a better understanding of the instantaneous values. The pressure sensor accuracy part indicates that the pressure sensors gives reasonable results but it is hard to draw any good conclusions.

From this study, it appears that it is possible to experimentally find an area that the mean propulsive pressure can be multiplied with to find the mean propulsive force of the swimmer. There is however a need for more experiments to get a better understanding of the possibility of using this method for propulsive force measurements.

Keywords: Swimming, Propulsive force, Power output, Repeatability analysis.

Acknowledgements

I would like to thank:

- My supervisor and examiner Martin Fagerström for assistance throughout the project.
- Maria Vitazka for lending and assisting with the **eo** SwimBETTTER force paddles.
- The team at TRACKS/FUSE for assistance with building the repeatability rig.
- Magnus Karlsteen for lending the force gauge.
- Gunnar Westman, Johan Setterberg and Johan Wallberg for valuable inputs regarding what has been done previously within force and power measurements.
- The swimmers that volunteered for the measurements.

Anton Wallin, Gothenburg, August 2024

List of Acronyms

Below is the list of acronyms that have been used throughout this thesis listed in alphabetical order:

bpm	Beats Per Minute
DPS	Distance Per Stroke
IMU	Inertial Measurement Unit
MAD	Measured Active Drag
NABA	Naval Architecture Based Approach
RMSE	Root Mean Square Error
rpm	Rotations Per Minute
SWUM	SWimming hUman Model
VPM	Velocity Perturbation Method
WA	World Aquatics

Contents

List of Acronyms	ix
List of Figures	xiii
List of Tables	xv
1 Introduction	1
1.1 Background	1
1.2 Purpose and goals	2
1.2.1 Limitations	2
2 Theory	3
2.1 Mechanics in swimming	3
2.1.1 Power and water resistance measurements in swimming	3
2.1.2 Power measurements in other sports	4
2.1.3 Force measurements in swimming	5
3 Reliability	7
3.1 Repeatability	7
3.1.1 Experiments	8
3.1.2 Data analysis	9
3.1.3 Results	9
3.2 Sensor accuracy	13
3.2.1 Experiments	13
3.2.2 Data analysis	13
3.2.3 Results	14
4 Initial force measurements	17
4.1 Initial measurements of forces and their correlations in fully tethered swimming	17
4.1.1 Experiments and setup	18
4.1.1.1 Data analysis	19
4.1.2 Results	20
5 Further force measurements	21
5.1 Testing equivalent area hypothesis on more swimmers	21
5.1.1 Method	21

5.1.2	Results	22
5.1.2.1	Swimmers with small comparison values	23
5.1.2.2	Swimmers with large comparison values	24
6	Conclusion	27
6.1	Repeatability and accuracy	27
6.2	Force and power measurements	28
6.2.1	Future work	28
	Bibliography	31
A	Instantaneous propulsive pressure	I

List of Figures

1.1	The figure shows how eo SwimBETTER handsets are mounted. . . .	1
3.1	The figure shows the repeatability rig used for the measurements. The crank is to the left and the "arms" are to the right.	7
3.2	The figure shows the rig assembled on the side of the pool that was used.	8
3.3	The figure shows where the handsets were mounted on the wooden hands compared to a handset mounted on my hand.	8
3.4	The figure shows a comparison between the regular mounting position (left) and the outer mounting position (right).	9
3.5	The figure shows how the cycle time t_{cycle} for the left handset varies for different measurement conditions. "Outer" denotes measurements with the outer mounting position and "changed" denotes measurements where the handsets changed hands.	10
3.6	The figure shows how the cycle time t_{cycle} for the right handset varies for different measurement conditions. "Outer" denotes measurements with the outer mounting position and "changed" denotes measurements where the handsets changed hands.	10
3.7	The figure shows how the mean cycle propulsive pressure $\bar{p}_{prop,c}$ for the left handset varies for different measurement conditions. "Outer" denotes measurements with the outer mounting position and "changed" denotes measurements where the handsets changed hands.	11
3.8	The figure shows how the mean cycle propulsive pressure $\bar{p}_{prop,c}$ for the right handset varies for different measurement conditions. "Outer" denotes measurements with the outer mounting position and "changed" denotes measurements where the handsets changed hands.	11
3.9	The figure shows the Δp values for both handsets.	14
3.10	The figure shows how the Δp values are distributed for both handsets.	14
4.1	The figure shows some of the equipment that were used for the measurements.	18
4.2	The figure shows the key parts of the setup. The left picture shows the force gauge connection and the right picture shows me swimming with a StrechCordz, eo SwimBETTER handsets, a front snorkel and a pull buoy.	19

4.3	The figure shows the results of the initial measurements as well as the least-square fit of a line corresponding to a constant A_e with a pull buoy. The k -value of the line is proportional to A_e	20
5.1	The figure shows the results of the measurements on the 8 swimmers as well as the least-square fit of a line corresponding to a constant A_e for each swimmer.	22
5.2	The figure shows the measurements on the 5 swimmers with small comparison values.	23
5.3	The figure shows the measurements on the 3 swimmers with large comparison values.	24
5.4	The figure shows the measurements on the 3 swimmers with large comparison values after the points determined as outliers have been removed.	25
A.1	The figure shows the p_{prop} profiles of the left handset "strokes".	II
A.2	The figure shows the p_{prop} profiles of the right handset "strokes".	III

List of Tables

3.1	The table shows some key dimensions of the test rig.	8
3.2	The table shows how the mean cycle time \bar{t}_{cycle} , the standard deviation σ_t and the t_{cycle} uncertainty σ_t/\bar{t}_{cycle} varies for different conditions. "Round 1" and "round 2" is the 100 bpm measurements performed during different days.	12
3.3	The table shows how the mean of the mean cycle propulsive pressure $\bar{p}_{prop,c}$, the standard deviation σ_p and the $\bar{p}_{prop,c}$ uncertainty $\sigma_p/\bar{p}_{prop,c}$ varies for different conditions. "Round 1" and "round 2" is the 100 bpm measurements performed during different days.	12
4.1	The table shows the settings used on the force gauge.	19
5.1	The table shows the RMSE value, the mean pressure span $\bar{p}_{prop,span}$ and the comparison value (RMSE/ $\bar{p}_{prop,span}$) for each swimmer.	23
5.2	The table shows the calculated value of A_e for the swimmers with low comparison values.	24
5.3	The table shows the determined value of A_e for the swimmers with larger comparison values after the determined outliers were removed.	25

1

Introduction

1.1 Background

In swimming, the goal is to finish a certain distance in the shortest possible time. To minimize the time, the average velocity should be maximized. This means that it is desired to maximize the propulsive force, and in turn the forward acceleration, while the forces in the other directions are kept low, since unnecessary large forces in these directions just means used energy that is not driving the swimmer forward. There exists some methods today to measure the propulsive force, power output and/or water resistance of a swimmer like Measured Active Drag (MAD) [3], Velocity Perturbation Method (VPM) [4] and Naval Architecture Based Approach (NABA) [5]. None of these methods does provide a simple way to measure the power output or propulsive force variations during training. Measuring continuous power or propulsive force output is something available today in cycling [6], cross-country skiing [7] and kayaking [8] but not for swimming.

Force paddles, like **eo** SwimBETTER [2], is a new technology introduced in swimming with the purpose to measure the force the swimmer is producing, as well as the direction of this force. These force paddles use built-in pressure sensors to measure the over-pressure on the palm of the hand, and use dedicated algorithms to determine the orientation of the hand to convert this pressure signal into a propulsive pressure signal. The **eo** SwimBETTER handsets mounted on a pair of hands are shown in Figure 1.1. The handsets are held in place by velcro straps.

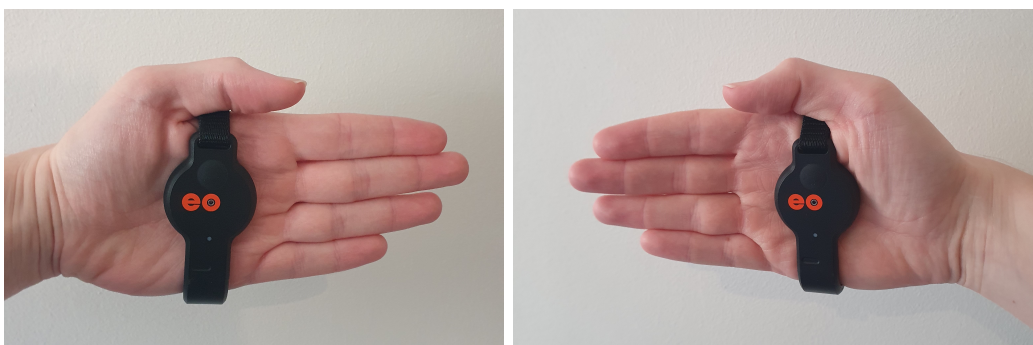


Figure 1.1: The figure shows how **eo** SwimBETTER handsets are mounted.

Even though the **eo** SwimBETTER handsets are called force paddles, they only measure the propulsive pressure p_{prop} for each hand and not the propulsive force. The propulsive pressure and its direction is usually enough for technique analysis

but there is a need to convert this propulsive pressure into a propulsive force in order to measure the power of a swimmer. To my knowledge, there is also a lack of independent reviews of the reliability of this type of force paddles. This means that there is a need to study the reliability of these force paddles to ensure that a potential power measurement method based on **eo** SwimBETTER handsets can be considered reliable.

1.2 Purpose and goals

The purpose of this project is to explore the possibility of using **eo** SwimBETTER force paddles to estimate the propulsive force of a swimmer, which later could lead into the development a novel power measurement method for swimming.

The first goal of the project is to validate the reliability of **eo** SwimBETTER force paddles. Both the accuracy and the precision of the paddles will be studied. The second goal is to develop and evaluate a method for how **eo** SwimBETTER force paddles can be used to measure the propulsive force of a swimmer. Measuring the propulsive force of a swimmer could result in a new method for measuring power output and water resistance that either can replace or complement existing power measurement methods like VPM.

1.2.1 Limitations

The precision part of this project is limited to comparing the mean propulsive pressure of "identical" strokes and puts less focus on the instantaneous propulsive pressure at different phases of a stroke. The accuracy part is limited to the accuracy of the pressure sensor in hydrostatic conditions and not in hydrodynamic conditions.

For the swimming performance measurement part, the focus will be on measuring the propulsive force of a swimmer and not the whole power measurement concept, since the propulsive force measurements needs to be solved before a whole power measurement method based on **eo** SwimBETTER force paddles can be developed.

This project is only focused on freestyle swimming but many parts could be applied to the other strokes as well.

2

Theory

2.1 Mechanics in swimming

The main force that a swimmer needs to overcome is the water resistance F_w that usually is considered to be proportional to the swimming velocity squared. Thus, it can be written as

$$F_w = Kv^2, \quad (2.1)$$

where K is a constant depending on the swimmer's size and technique, and v is the velocity of the swimmer [9]. If the swimmer has a constant velocity (no acceleration) Newtons first law says that the swimmer is in force equilibrium, meaning that

$$F_p = F_w, \quad (2.2)$$

where F_p is the propulsive force of the swimmer. The power output P of the swimmer is

$$P = \vec{F} \cdot \vec{v} = (F_p, F_t, F_v) \cdot (v, 0, 0) = F_p v = Kv^3, \quad (2.3)$$

where \vec{F} is the force vector from the swimmer, \vec{v} is the velocity vector of the swimmer, F_t is the transverse force and F_v is the vertical force from the swimmer. After time-averaging the time-dependent quantities P and v into the average power output \bar{P} and the average velocity \bar{v} , the equation can be rewritten as

$$\bar{v} = \sqrt[3]{\frac{\bar{P}}{K}}. \quad (2.4)$$

From this it is possible to see that \bar{P} should be maximized and K should be minimized to obtain the largest \bar{v} . Therefore, the values of K and \bar{P} (or \bar{F}_p since $\bar{P} = \bar{F}_p \bar{v}$) are interesting to measure since they influence the swimming velocity and ultimately the finish time. \bar{v} can easily be measured by measuring the time it takes to swim a predetermined distance with a stopwatch or video analysis. There is only one equation but two unknowns (\bar{P} and K) meaning that we do not have enough information for determining these unknowns. That means that different methods have to be used to determine these unknowns.

2.1.1 Power and water resistance measurements in swimming

One method that has been introduced to measure \bar{P} and K is the Measured Active Drag (MAD) method [3]. This method uses fixed grips placed in the water that the

swimmer grips onto while performing the pulling phase of the stroke. The applied force to the grip is measured and no propulsive force is generated by the arm moving through the water, since the arm is held stationary in the water by the grips. By using force equilibrium the water resistance of the swimmer can be calculated for different velocities, meaning that K can be determined. A disadvantage with this method is that this system is large and hard to use in everyday training. The stationary grips do also change the stroke since there is no need to catch the water during the stroke.

Another method introduced is the Velocity Perturbation Method (VPM) [4]. The basis for this method is that a small disturbance (a perturbation) to the velocity is introduced by having the swimmer tow a raft with a known water resistance. By measuring the maximum velocity with and without the raft, and then assuming that the power output is the same in both tests, \bar{P} and K can be calculated since the swim with the raft provides an additional equation. This method is much more portable but it can only measure the peak power output since the swimmer needs to be rested to be able to provide the same power output during both tests.

A newer method similar to VPM is the Naval Architecture Based Approach (NABA) [5]. Like the VPM the swimmers velocity is disturbed by a force, but this time the force is towing the swimmer to a higher speed than the free swimming velocity. The theory behind this method is that the swimmers body is thought of as the hull of a ship and the arms as the propeller. The drag of the "hull" without any active swimming (passive drag) can be measured by towing the passive swimmer at different speeds and measuring the towing force. By assuming equal power as well as equal Distance Per Stroke (DPS) (meaning that the frequency increases when the velocity increases) the drag of the swimmer (active drag) can be calculated. This method has the advantage of much lower uncertainty, but like VPM it can only measure the peak power and not the current power while swimming.

A problem with VPM and NABA is that they only enable the measurement of maximum power while rested and not the measurement of current power during training or maximum power while fatigued. Therefore it is interesting to turn to other sports where such power measurements are performed today.

2.1.2 Power measurements in other sports

A sport where power measurements are much more common is cycling. The most common approach is to use strain gauges in the drive-chain to measure the torque produced by the cyclist. By measuring this torque and the angular velocity, the power of the cyclist can be calculated [10]. The introduction of power meters in cycling has for example enabled studies of power profiles during a race [11] and measurements of the power a cyclist can produce depending on the frequency [12].

Another type of sport where power measurements have been introduced is rowing and kayaking. The mechanics of kayaking are similar to the mechanics of swimming, since both are based on propulsion in water and the propulsive forces are cyclic. These force variations means that the instantaneous velocity varies around an average velocity that is the velocity most often used when measuring power. The propulsive power is measured by strain gauges in the paddle handle that measure

the propulsive force produced by the athlete and either GPS or video analysis is used to determine the velocity [13] [14].

In cross-country skiing the company Skisens, based on a Chalmers project, have introduced a solution similar to the kayaking solution where strain gauges are installed in the ski pole handles to measure the force in the poles. An Inertial Measurement Unit (IMU) is used to determine the angle of the pole to determine how much of the force is propulsive and a GPS system is used to determine the velocity of the athlete [7].

2.1.3 Force measurements in swimming

In order to be able to apply the power measurement method used today in kayaking and cross-country skiing to swimming we need to know what propulsive forces we want to measure. The current focus is only on the arms since the arms produce more propulsion than the legs and are easier to work with [15]. When the swimmer performs a stroke the pressure increases on the palm of the hand while the pressure decreases on the back of the hand. This results in a pressure difference that in turn results in a force propelling the swimmer [16]. To know how large the propulsive force is during the stroke there is a need to know the pressure difference between the palm and the back of the hand as well as the orientation of the hand in order to determine how much of this force is propulsive.

It is possible to measure this pressure difference by placing pressure sensors on both sides of the hand and then using video analysis to determine the hand orientation. It is however important to note that the pressure difference from each place in the hand has a different contribution to the mean pressure across the hand, which is the interesting pressure to know to determine the propulsive force without covering the whole hand with pressure sensors [16] [17]. The commercially available product Aquanex [18] appears to work in this way. Since this alternative has wired connections to the pressure sensors and rely on external video analysis to determine the hand orientation they appear more suited for research than for everyday use in training.

There is however a newer alternative that claims to be able to measure this propulsive force in an easier way, which seems suitable for everyday use in training. The solution is to have handsets with pressure sensors as well as an IMU with an accelerometer and a gyroscope that can calculate the path of the hand and the hand orientation during the stroke. Two commercial products have been launched, the Trainesense SmartPaddle (appears to be discontinued) and the **eo** SwimBETTER [2]. Both these products collect the IMU and pressure sensor data while swimming, and then transfer the data to a smartphone app after the swim.

It has been shown that IMUs could be used to create a reliable system for calculating the orientation of the hand during the stroke [19]. There is not however that many studies performed where the accuracy of the commercial handsets have been tested and no one appears to have studied the repeatability of these handsets or the repeatability of this method as a whole. When the SmartPaddle was compared to the Aquanex system both systems produced similar results [20]. These results are promising but it is uncertain if the Aquanex system can be considered as a "golden

2. Theory

standard". When comparing the propulsive force from a strain gauge in a kayak paddle with the propulsive force from a SmartPaddle sensor mounted on the paddle blade the results are similar [21].

3

Reliability

The first part of this project is done by looking at two key metrics for determining how a measured value compares to the true value, the precision and the accuracy. The precision describes how repeatable a measurement is, or in other words how large the difference is between different measurements with the same conditions. The accuracy describes how close a measurement is to the true value [22].

The optimal way of determining how reliable the handsets are would probably be to use a "mechanical twin" of a swimmer that can perform the stroke and measure the forces in the joints. An example of a mechanical twin known as SWimming hUman Model (SWUM) exists, but it has a very complex system of joints to recreate a regular swimming stroke [23]. This is considered to be too complex to implement in this project meaning that other methods have to be used. The selected parts that were studied in project were the repeatability of the mean propulsive pressure and the accuracy of the pressure sensors.

3.1 Repeatability

For this part a rig that could repeat the same "stroke" many times had to be constructed and tested. The main requirements was that this "stroke" should follow the same path time after time, that this "stroke" should resemble a regular swim stroke (entry, pull, exit and recovery phases) and that the handsets could be mounted on the rig. It was decided that the rig would be cranked manually since an electric drive system would require an electric motor with a very high torque at low angular velocities or the use of a large gearbox between the motor and the axle. This is due to that the rig would require a very large torque at a low angular velocity. The rig that was built is shown in Figure 3.1.



Figure 3.1: The figure shows the repeatability rig used for the measurements. The crank is to the left and the "arms" are to the right.

The rig is built around an axle held

up by a wooden frame and ball bearings. On one side of the axle two "arms" are mounted and on the other side a crank is placed. On the ends of the "arms" wooden hands are mounted. Some key dimensions of the rig are shown in Table 3.1.

Table 3.1: The table shows some key dimensions of the test rig.

Axle height over water line	40 cm
Length from axle to tip of the hand	65 cm
Length from axle to eo SwimBETTER placement	60 cm

To use the rig the wooden frame was clamped to the pool wall and eo SwimBETTER handsets were fixed to the wooden hands with the velcro straps. This assembly is shown in Figure 3.2.



Figure 3.2: The figure shows the rig assembled on the side of the pool that was used.

3.1.1 Experiments

The measurements were performed according to the following points:

- With the eo SwimBETTER handsets mounted on the wooden hands according to Figure 3.3, the crank was used to rotate the axle and the paddle arms. This meant that the wooden hands moved through the water similar to a regular stroke following the same path multiple times.
- To help with keeping the same cycle time a metronome from Google [24] was used.
- The metronome was set to 60, 80 or 100 Beats Per Minute (bpm) and I tried to keep a cycle time such that a wooden hand hits the water at every beep. This means that 60 bpm should be



Figure 3.3: The figure shows where the handsets were mounted on the wooden hands compared to a handset mounted on my hand.

30 Rotations Per Minute (rpm), 80 bpm should be 40 rpm and 100 bpm should be 50 rpm.

- The rig was cranked for around 1 minute every time.

A total of 4 measurements were performed for each metronome setting (60, 80 and 100 bpm). Additionally, 4 measurements were performed at 100 bpm where the **eo** SwimBETTER handsets had been mounted 2 cm further out on the wooden hands as shown in Figure 3.4, 4 measurements were performed at 100 bpm where the left and right handsets switched places and 4 measurements were performed at 100 bpm during another day just to ensure that the measurements are independent on which day they were performed.



Figure 3.4: The figure shows a comparison between the regular mounting position (left) and the outer mounting position (right).

3.1.2 Data analysis

The first part of analysing the data is to determine where each "stroke" starts and ends. The chosen definition is that a "stroke" starts (time t_1) when $p_{prop} > 0.2$ kPa, that the pull phase ends (time t_2) when $p_{prop} < 0.2$ kPa and that the whole "stroke" ends (time t_3) when the next stroke starts (t_1 of the next "stroke"). For comparison, the maximum p_{prop} during a stroke was usually between 2.5 and 4 kPa depending on setup. The cycle time t_{cycle} is then calculated as

$$t_{cycle} = t_3 - t_1, \quad (3.1)$$

and the mean cycle propulsive pressure $\bar{p}_{prop,c}$ is calculated as

$$\bar{p}_{prop,c} = \frac{1}{t_3 - t_1} \int_{t_1}^{t_3} p_{prop} dt \quad (3.2)$$

where the integral is evaluated with the trapezoidal rule. The mean and the standard deviation of t_{cycle} and $\bar{p}_{prop,c}$ are calculated for each setup to give a value of how much t_{cycle} and $\bar{p}_{prop,c}$ vary between strokes that should be more or less identical. All "strokes" for each setup are combined for this except for the first 5 "strokes" of each measurement. The first 5 "strokes" were removed since the pool water is stationary before a measurement, but then starts moving as the rig rotates its first rotations. The variations of t_{cycle} and $\bar{p}_{prop,c}$ are the metrics most important for the reliability of a method for determining the propulsive force of a swimmer with **eo** SwimBETTER handsets so those are the metrics in focus here.

It is also possible to compare the p_{prop} profile during the pull phase (between t_1 and t_2) for different strokes. This is outside the scope of this project but some figures of this is shown in Appendix A.

3.1.3 Results

The cycle time variations are shown in Figure 3.5 (left handset) and Figure 3.6 (right handset). As expected, it can be seen that the measurements with 60 and 80 bpm

have longer cycle times.

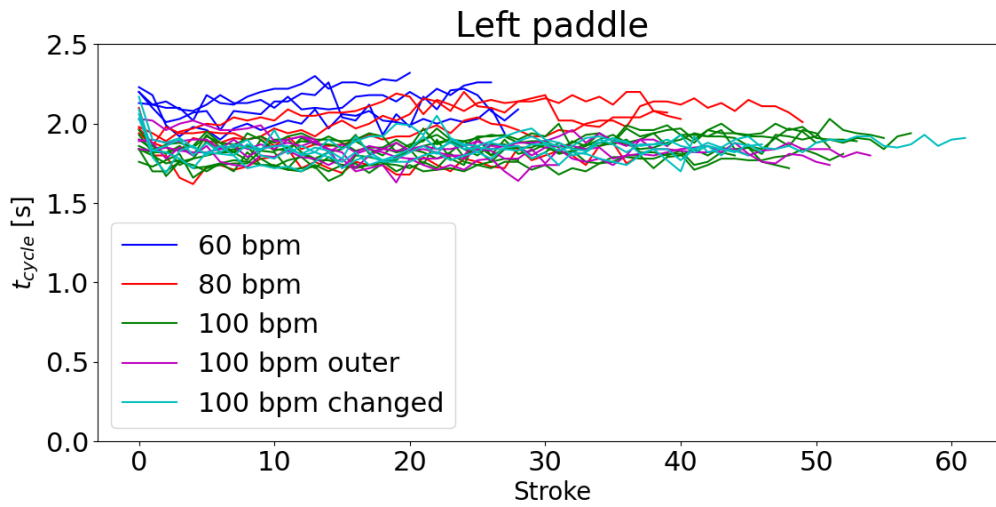


Figure 3.5: The figure shows how the cycle time t_{cycle} for the left handset varies for different measurement conditions. "Outer" denotes measurements with the outer mounting position and "changed" denotes measurements where the handsets changed hands.

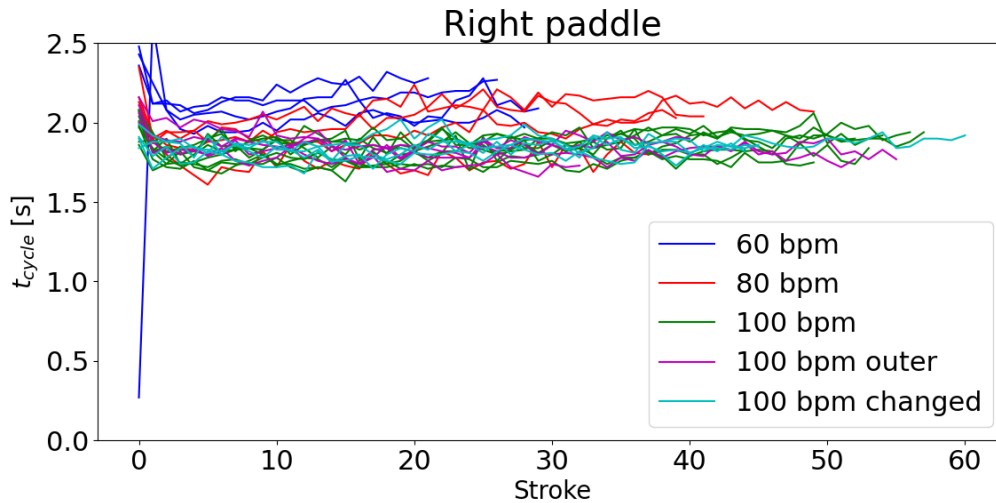


Figure 3.6: The figure shows how the cycle time t_{cycle} for the right handset varies for different measurement conditions. "Outer" denotes measurements with the outer mounting position and "changed" denotes measurements where the handsets changed hands.

The mean cycle propulsive pressures $\bar{p}_{prop,c}$ are shown in Figure 3.7 (left handset) and Figure 3.8 (right handset). As expected, it can be seen that the measurements with 60 and 80 bpm resulted in lower values, since the handsets in these cases are moving slower through the water. It can also be seen that the outer handset position

resulted in higher values, especially for the right paddle, and this is also reasonable since the outer position has a longer radius of rotation meaning that the velocity through the water is higher.

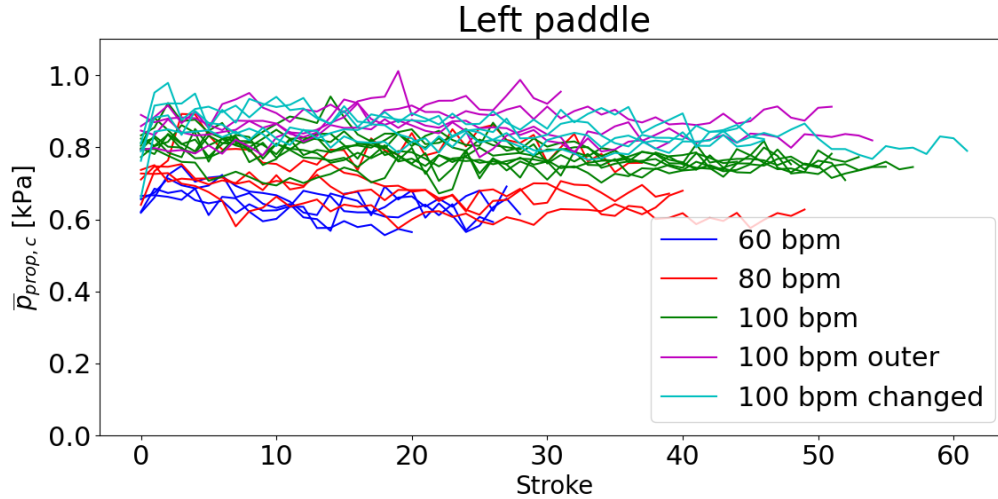


Figure 3.7: The figure shows how the mean cycle propulsive pressure $\bar{p}_{prop,c}$ for the left handset varies for different measurement conditions. "Outer" denotes measurements with the outer mounting position and "changed" denotes measurements where the handsets changed hands.

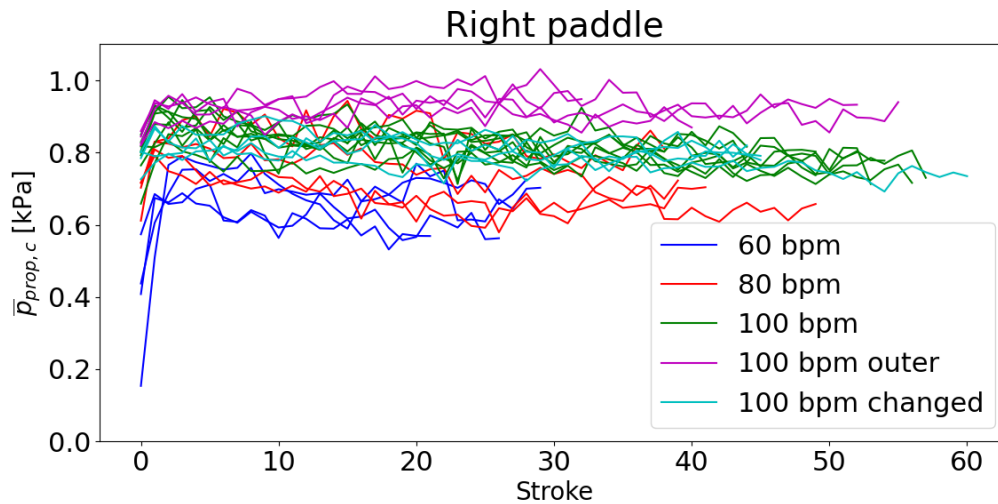


Figure 3.8: The figure shows how the mean cycle propulsive pressure $\bar{p}_{prop,c}$ for the right handset varies for different measurement conditions. "Outer" denotes measurements with the outer mounting position and "changed" denotes measurements where the handsets changed hands.

The mean \bar{t}_{cycle} , standard deviation σ_t and uncertainty σ_t/\bar{t}_{cycle} of the cycle time t_{cycle} for the different setups are shown in Table 3.2. It can be seen that the uncertainties are between 3.0 % and 7.5 % depending on setup, and that the 100

3. Reliability

bpm setups have the lower uncertainties. It can also be seen that \bar{t}_{cycle} varied a lot between the days for the 100 bpm measurements.

Table 3.2: The table shows how the mean cycle time \bar{t}_{cycle} , the standard deviation σ_t and the t_{cycle} uncertainty σ_t/\bar{t}_{cycle} varies for different conditions. "Round 1" and "round 2" is the 100 bpm measurements performed during different days.

	Left handset			Right handset		
	\bar{t}_{cycle} [s]	σ_t [s]	σ_t/\bar{t}_{cycle} [-]	\bar{t}_{cycle} [s]	σ_t [s]	σ_t/\bar{t}_{cycle} [-]
60 bpm	2.1148	0.0992	0.0469	2.1123	0.0948	0.0449
80 bpm	1.9754	0.1429	0.0723	1.9725	0.1469	0.0745
100 bpm round 1	1.7897	0.0641	0.0358	1.7894	0.0656	0.0367
100 bpm round 2	1.8808	0.0609	0.0324	1.8804	0.0611	0.0325
100 bpm outer	1.8257	0.0622	0.0341	1.8258	0.0644	0.0353
100 bpm change	1.8442	0.0571	0.0309	1.8448	0.0565	0.0306

The mean $\bar{p}_{prop,c}$, standard deviation σ_p and uncertainty $\sigma_p/\bar{p}_{prop,c}$ of the mean cycle propulsive pressure $\bar{p}_{prop,c}$ for the different setups are shown in Table 3.3. It can be seen that the uncertainties are between 3.8 % and 11.6 %, and when comparing the uncertainties in Table 3.2 with the uncertainties Table 3.3, it can be seen that a lower t_{cycle} uncertainty can be connected to a lower $\bar{p}_{prop,c}$ uncertainty. As noted earlier, a lower bpm is connected to a lower $\bar{p}_{prop,c}$, while the outer handset position is connected to a higher $\bar{p}_{prop,c}$. It can be seen that the right handset has a higher $\bar{p}_{prop,c}$ for all setups, except when the handsets changed hands. For that setup the left handset has a higher $\bar{p}_{prop,c}$. This indicates that the two hands of the rig are not identical and that this asymmetry is the reason for different $\bar{p}_{prop,c}$ for the handsets. Thus, this difference does not appear to be caused by differences between the two handsets. The $\bar{p}_{prop,c}$ difference between the different days ("round 1" and "round 2") is smaller than the \bar{t}_{cycle} difference indicating that the values do not depend on when the measurements are performed.

Table 3.3: The table shows how the mean of the mean cycle propulsive pressure $\bar{p}_{prop,c}$, the standard deviation σ_p and the $\bar{p}_{prop,c}$ uncertainty $\sigma_p/\bar{p}_{prop,c}$ varies for different conditions. "Round 1" and "round 2" is the 100 bpm measurements performed during different days.

	Left handset			Right handset		
	$\bar{p}_{prop,c}$ [kPa]	σ_p [kPa]	$\sigma_p/\bar{p}_{prop,c}$ [-]	$\bar{p}_{prop,c}$ [kPa]	σ_p [kPa]	$\sigma_p/\bar{p}_{prop,c}$ [-]
60 bpm	0.6348	0.0378	0.0595	0.6574	0.0608	0.0924
80 bpm	0.6856	0.0691	0.1008	0.7275	0.0839	0.1154
100 bpm round 1	0.7746	0.0403	0.0521	0.8252	0.0409	0.0496
100 bpm round 2	0.7768	0.0358	0.0460	0.7990	0.0454	0.0568
100 bpm outer	0.8659	0.0429	0.0496	0.9286	0.0354	0.0381
100 bpm change	0.8429	0.0381	0.0452	0.8004	0.0382	0.0477

3.2 Sensor accuracy

The natural way of testing the pressure sensor accuracy would be to compare the pressure readings of stationary handsets to the expected hydrostatic pressure at different depths, which is very similar to what has been done in [25]. This is however impossible to do here since the raw pressure data is hidden by the algorithms presenting the results. The only available data is the pressure difference between the two pressure sensors. The algorithm also requires that at least three strokes are performed during a test to produce any reading. These constraints meant that the sensor accuracy evaluation method had to be adapted to produce a usable result.

The difference in hydrostatic pressure Δp is

$$\Delta p = \rho g \Delta h, \quad (3.3)$$

where g is the gravitational acceleration and Δh is the height difference [26]. This means that holding the handsets under water in such a way that the two pressure sensors are at different depths should result in a pressure difference between the two sensors. This meant that a method where the handsets are held under water that also follows the constraints needed to be developed.

3.2.1 Experiments

While standing on the bottom of the pool with the **eo** SwimBETTER handsets mounted on the hands, the arms were submerged into the water such that the fingers are pointing out into the pool and the little fingers towards the bottom of the pool. This means that the side pressure sensor is closer to the bottom than the palm pressure sensor, and thereby experiences a higher pressure. The hands were then rotated very very slowly back and forth around the axis from the elbow to the fingertips in order to activate the readings and to get the maximum depth separation between the pressure sensors. The rotations were performed as slowly as possible to minimize the effects of hydrodynamics and just get the hydrostatic pressures. After a few rotations I finally pushed off the wall and swam one length in the pool to register the measurement. This procedure was repeated a total of 16 times.

The distance between the two pressure sensors is about 5 cm, meaning that $\Delta h \approx -5$ cm while the hand is held with the little finger downwards (since $\Delta p = p_{palm} - p_{side}$ and the p_{palm} sensor is above the p_{side} sensor in the water). This means that Δp is expected to be close to -0.5 kPa ($\rho \approx 1000$ kg/m³ and $g \approx 9.82$ m/s²).

3.2.2 Data analysis

The first part of the data analysis is to calculate Δp for the handsets from the total pressure curves. To do this, a 2nd degree polynomial was fitted to the total pressure curve around a local minimum of this curve. The minimum of this 2nd degree polynomial is then used as the Δp value for this local minimum of the curve. This procedure is performed for all local minima that were suitable for fitting a 2nd degree polynomial. Furthermore, all values is the $-0.65 < \Delta p < -0.35$ kPa range

were considered valid measurements. This was done to avoid measurements where the source of the peak is unknown. For example, it could be caused by not rotating far enough to obtain the maximum sensor separation before rotating back, or by not pointing the fingers in the correct direction.

3.2.3 Results

A total of 47 valid measurements were found for the left handset, while a total of 44 valid measurements were found for the right handset. The Δp values for these measurements are shown in Figure 3.9, and a histogram of the measurements are shown in Figure 3.10.

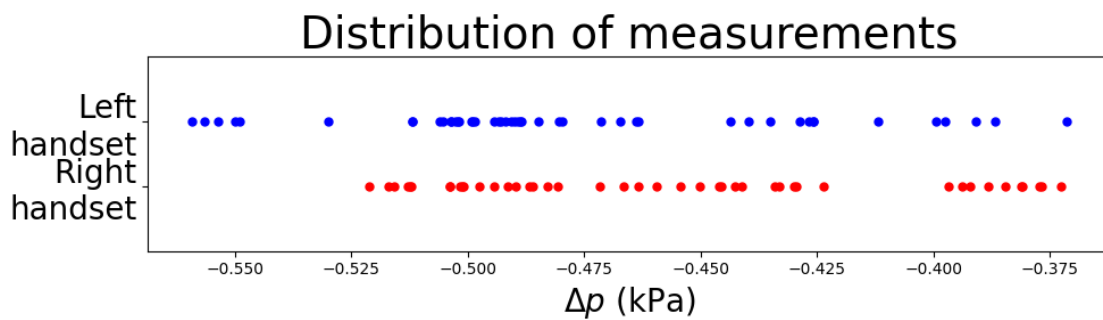


Figure 3.9: The figure shows the Δp values for both handsets.

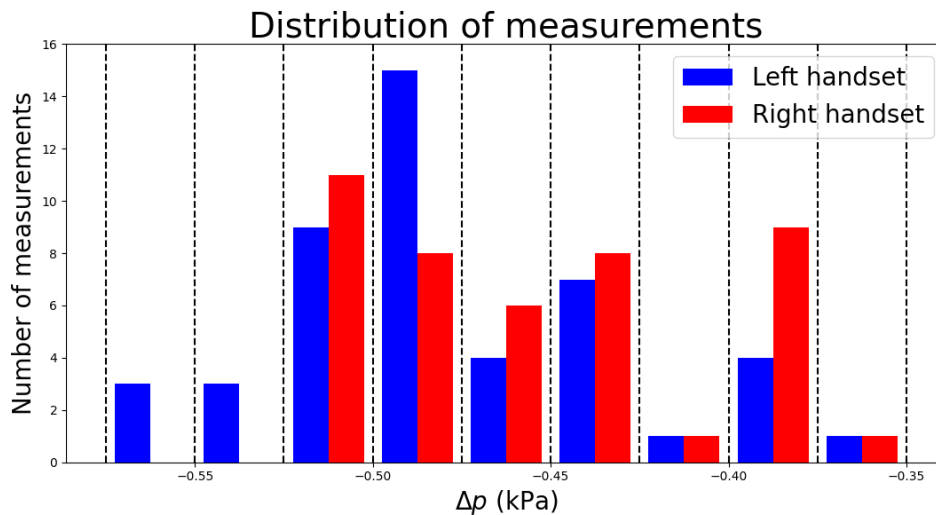


Figure 3.10: The figure shows how the Δp values are distributed for both handsets.

The distributions for the handsets are not close to a normal distribution and it does not appear that the distributions will approach a normal distribution with many more measurements. The means are -0.478 kPa for the left handset and -0.456 kPa for the right handset. The standard deviations are 0.046 kPa for the left handset and 0.047 kPa for the right handset. It can be seen that the means

of both handsets are fairly close to the expected value of ≈ -0.5 kPa, but the standard deviations are fairly large. This can also be seen in the figures where the measurements are distributed in the -0.56 to -0.37 kPa range, and not gathered in a smaller range. It can be noted that the highest stacks are found close to the expected value, and that no values below -0.56 kPa were found while many values above the expected value were found.

One possible interpretation of the observed distribution is that the cutoff for removing measurements from incomplete rotations was set too high. Removing more values without knowing which rotations were incomplete would however force the result to say that the sensors are accurate since this would mean that only the measurements that says that the sensors are accurate (Δp close to -0.5 kPa) will be kept. This means that this part is inconclusive since it is impossible to say if the deviating values are caused by sensor inaccuracy or a poor method. The obvious solution to get a better result is to use the raw pressure sensor reading at different depths instead of the difference between the sensors, but this would require access to the raw pressure sensor readings which were unavailable for me during this project.

4

Initial force measurements

4.1 Initial measurements of forces and their correlations in fully tethered swimming

In this part, the goal was to study the correlation between the forces involved in fully tethered swimming. Fully tethered swimming means that the swimmer is held stationary in the water by a line, and one force involved in fully tethered swimming is the force in this line. This instantaneous force is denoted F_{line} and its time-average is \bar{F}_{line} . Another force involved is the mean propulsive force produced by the swimmers arms, called $\bar{F}_{arm,prop}$. This force can not be measured directly, but the mean propulsive pressure \bar{p}_{prop} of the arms can be calculated from the force paddle data. Dimensional analysis gives that a pressure should be multiplied by an area to get a force. This area is here called the "equivalent area" A_e of a swimmers arm and this means that the mean propulsive force can be calculated as

$$\bar{F}_{arm,prop} = A_e \bar{p}_{prop}. \quad (4.1)$$

Stationary swimming means that the swimmer does not experience any water resistance forces. Newton's first law [27] then says that force equilibrium is needed for the swimmer to remain stationary. The only forces acting on the swimmer in the swimming direction is the force in the line and the propulsive force of the swimmer. If the legs do not provide any propulsive force the total propulsive force is equal to the propulsive force from the arms such that

$$\bar{F}_{line} = \bar{F}_{arm,prop} = A_e \bar{p}_{prop}. \quad (4.2)$$

Since \bar{F}_{line} and \bar{p}_{prop} can be measured it is possible to determine A_e for fully tethered swimming. Since A_e is the area used for forward propulsion while swimming, and the arm does not change its volume, a reasonable hypothesis is that A_e is independent of effort level. If this hypothesis holds it would be reasonable to assume that an athlete has the same A_e during free swimming. By using this assumption it is then possible to calculate the mean propulsive force during free swimming $\bar{F}_{arm,free}$ as

$$\bar{F}_{arm,free} = A_e \bar{p}_{prop,free}, \quad (4.3)$$

where $\bar{p}_{prop,free}$ is the mean propulsive pressure during free swimming. This would mean that power measurements could be performed in swimming in a very similar way of what is being done today in kayaking and cross-country skiing, by measuring the velocity and the propulsive pressure, and then converting the latter to a propulsive force.

It should be noted that, with this method, A_e is calculated based on the pressure difference between the palm of the hand and the side of the hand (where the pressure should be equal to the hydrostatic pressure). It is expected that the pressure on the back of the hand is lower than the hydrostatic pressure, meaning that the pressure difference across the hand is larger than the measured pressure difference. This means that the true propulsive area is smaller than the measured A_e . On the other hand, the whole arm can not be used for propulsion at the start and end of the pull phase, meaning that the propulsive area in the middle of the pull phase when the whole arm can be used is larger than the averaged area. These parts should not change the order of magnitude of A_e compared to the area of an arm, only change it by a small factor.

If the setup is changed from no leg movements to the swimmer performing a flutter kick with their legs that produces the mean propulsive force $\bar{F}_{flutter}$ the force equilibrium instead becomes

$$\bar{F}_{line} = \bar{F}_{arm,prop} + \bar{F}_{flutter} = A_e \bar{p}_{prop} + \bar{F}_{flutter}. \quad (4.4)$$

Since A_e is only related to the arms of a swimmer, it should be independent of the swimmer using a flutter kick or not. This means that the hypothesis is that the same \bar{p}_{prop} should result in a higher \bar{F}_{line} but that there will be larger variations depending on the flutter kick effort level compared to the arm effort level.

4.1.1 Experiments and setup

Since this part was mostly performed as "trial and error" there was not any predetermined number of tests performed or any predetermined speeds/intensities used. The method described below is the method used in the experiments that resulted in the results presented in this report. I performed the tests on myself. Some of the equipment used is shown in Figure 4.1.

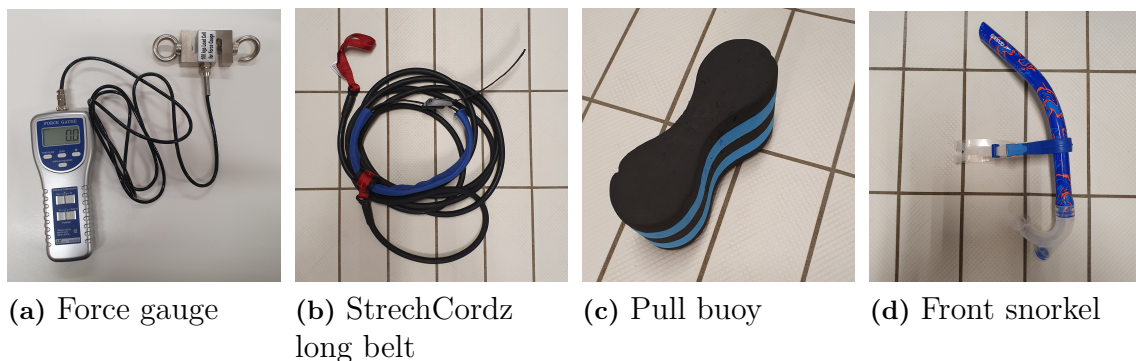


Figure 4.1: The figure shows some of the equipment that were used for the measurements.

The force sensor on the force gauge, a Lutron FG-5100, was connected to the backstroke handles of a starting block with a lashing strap, and the loop on the red StretchCords long belt [28] elastic band was connected to the force sensor. The force

gauge was connected by cables to a laptop. The belt of the StrechCordz was fixed around my waist and I wore the **eo** SwimBETTER handsets, a front snorkel and a pull buoy. The pull buoy was used to minimize flutter kicking and the front snorkel to simplify breathing. This setup is shown in Figure 4.2.



Figure 4.2: The figure shows the key parts of the setup. The left picture shows the force gauge connection and the right picture shows me swimming with a StrechCordz, **eo** SwimBETTER handsets, a front snorkel and a pull buoy.

The settings used on the force gauge are shown in Table 4.1.

Table 4.1: The table shows the settings used on the force gauge.

Measurement type	Normal Measurement (continuous measurements)
Sampling time	Fast (≈ 0.2 s)
Force unit	Newton

Each measurement was performed according to the following procedure:

- With the computer recording the force gauge readings and the **eo** SwimBETTER handsets recording, I pushed off the wall and started swimming freestyle at a chosen intensity level.
- Once I became stationary due to the increased resistance from the StrechCordz, I tried to maintain the same position for at least 10 strokes (5 cycles).

I performed a total of 10 tests with these instructions at different intensities from easy swimming to close to maximum effort. Additionally, 7 tests were performed where I swam without a pull buoy and instead performed a flutter kick with the legs to see how this change would influence the values of \bar{F}_{line} and \bar{p}_{prop} .

4.1.1.1 Data analysis

To get usable data from a test there is a need to calculate \bar{p}_{prop} and \bar{F}_{line} . \bar{p}_{prop} is calculated by integrating the $p_{prop,right}$ and $p_{prop,left}$ curves over a selected time interval and then dividing by the interval length. The interval was set to be two or three whole stroke cycles (four or six strokes) where t_1 is the start of the interval and t_2 is the end of the interval. This meant that \bar{p}_{prop} is calculated as

$$\bar{p}_{prop} = \frac{1}{t_2 - t_1} \left(\int_{t_1}^{t_2} p_{prop,right} dt + \int_{t_1}^{t_2} p_{prop,left} dt \right), \quad (4.5)$$

where the integrals were evaluated with the trapezoidal rule. To calculate \bar{F}_{line} the mean of the F_{line} curve values in the t_1 to t_2 interval is taken as the value of \bar{F}_{line} . Visual inspection was used to ensure that the F_{line} curve is more or less constant in the interval, to ensure that the swimmer is stationary. To determine how well the least-square fit line fits to the measurement data, the Root Mean Square Error (RMSE) is calculated [29]. This is done by

$$\text{RMSE} = \sqrt{\frac{1}{n} \sum_{i=1}^n (\bar{F}_{line,i} - A_e \bar{p}_{prop,i})^2}, \quad (4.6)$$

where n is the number of measurements.

4.1.2 Results

The results of these measurements are shown in Figure 4.3. As expected it can be seen that a higher \bar{p}_{prop} correlates to a higher \bar{F}_{line} when a pull buoy is used. It can also be seen that \bar{F}_{line} appears to be proportional to \bar{p}_{prop} meaning that A_e seems to be constant over this effort range. A least-square fit of the measurements with a pull buoy gives that $A_e = 3.136 \text{ dm}^2$ and the RMSE value is 5.967 N. The A_e value seems reasonable since it has the same order of magnitude as the area as the hand and lower arm.

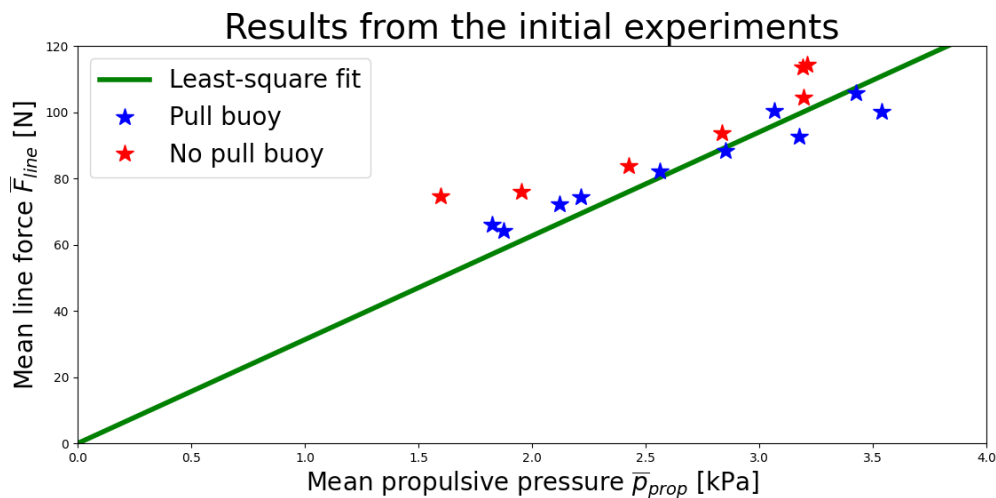


Figure 4.3: The figure shows the results of the initial measurements as well as the least-square fit of a line corresponding to a constant A_e with a pull buoy. The k -value of the line is proportional to A_e .

When looking at the measurements without a pull buoy it can be seen that all \bar{F}_{line} values are larger than the \bar{F}_{line} value expected from the \bar{p}_{prop} value (the green line is the expected \bar{F}_{line} value). This is what is expected since the legs provide an extra propulsive force $\bar{F}_{flutter}$ to the force equilibrium. The flutter kick effort level was not written down since this was preliminary testing meaning that it is impossible to evaluate if the data points furthest from the green line are the points with the highest flutter kick effort level.

5

Further force measurements

5.1 Testing equivalent area hypothesis on more swimmers

Given the preliminary data presented in Chapter 4, it seems reasonable to assume that an equivalent area can be used to calculate $\bar{F}_{arm,prop}$ from \bar{p}_{prop} . To explore this further, similar tests were made on 8 competitive swimmers, 5 males and 3 females aged 18-25 years old, with at least 450 World Aquatics (WA) swimming points in the 100 m LCM freestyle (equivalent to personal bests faster than 1:01.15 s for males and 1:07.47 s for females [30]). All participants provided oral consent for participation.

5.1.1 Method

The procedure for the measurements were as follows:

- Each athlete performed at least 500 m swimming before starting the tests but no standardized warm-up was used since these tests do not require the athletes to perform at peak physical performance.
- An identical setup with the force gauge, **eo** SwimBETTER handsets, a front snorkel and a pull buoy was used as the one presented in Chapter 4.
- A green StrechCordz long belt was used instead of the stiffer red StrechCordz long belt used earlier. This was due to availability at the pool used for these measurements.
- The swimmer was asked to perform 6 fully tethered swims where they push off the wall, swim freestyle until they stop moving forward and then perform 10 strokes (5 cycles) while stationary.
- The swimmer was asked to perform measurements 1 and 4 at an effort corresponding to speed 2, measurements 2 and 5 at an effort corresponding to speed 3 and measurements 3 and 6 at an effort corresponding to speed 4, using a speed scale where speed 1 is easy swim and speed 5 is maximum effort.
- No measurements without a pull buoy were performed.

A measurement took around 20 s of active swimming time and the next measurement was started as soon as the swimmer felt ready, which usually meant that a new measurement was started every 60-90 s as long as there was not any issues like **eo** SwimBETTER handsets falling off. This meant that the total time for each swimmer was around 15 min including instruction time before and data saving time after each swimmer.

The data analysis was performed in the same way as in the initial experiments, meaning that \bar{p}_{prop} was calculated by integrating the $p_{prop,right}$ and $p_{prop,left}$ curves over a selected time interval corresponding to two whole cycles (four strokes) and \bar{F}_{line} was calculated by taking the mean of the points on the F_{line} curve in that time interval.

5.1.2 Results

The results for the 8 swimmers are shown in Figure 5.1. Subject Female 2 only has 5 data points since one measurement did not give any result, and this was not caught in time to redo that measurement.

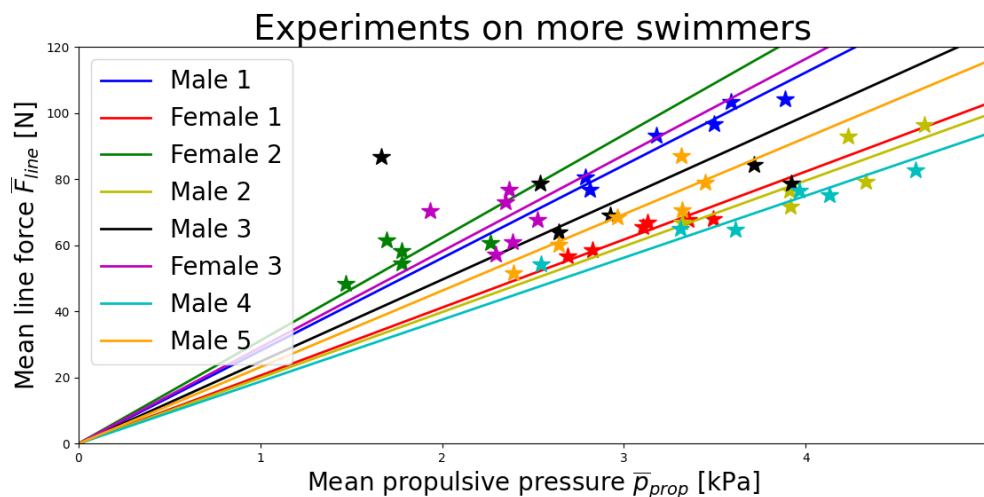


Figure 5.1: The figure shows the results of the measurements on the 8 swimmers as well as the least-square fit of a line corresponding to a constant A_e for each swimmer.

In Table 5.1 the RMSE value, the difference between the highest and lowest \bar{p}_{prop} (called the mean pressure span $\bar{p}_{prop,span} = \bar{p}_{prop,max} - \bar{p}_{prop,min}$) and the fraction $RMSE/\bar{p}_{prop,span}$ (called the comparison value) are shown for each swimmer. The comparison value is low for a good fitting line since it says that the fitting error (RMSE) is low while the measurements have a large mean pressure span ($\bar{p}_{prop,span}$ becomes large). This means that the comparison value can be used for determining if the measurements fit well to the equivalent area hypothesis.

Table 5.1: The table shows the RMSE value, the mean pressure span $\bar{p}_{prop,span}$ and the comparison value ($RMSE/\bar{p}_{prop,span}$) for each swimmer.

Swimmer	RMSE value [N]	$\bar{p}_{prop,span}$ [kPa]	Comparison value [N/kPa]
Male 1	3.104	1.096	2.831
Female 1	2.092	0.799	2.617
Female 2	6.198	0.796	7.791
Male 2	5.459	1.331	4.101
Male 3	21.338	2.257	9.454
Female 3	8.986	0.592	15.179
Male 4	3.692	2.057	1.795
Male 5	5.188	1.055	4.918

By using the comparison value for each swimmer the swimmers can be divided into two groups, one with small comparison values and one with large comparison values. The chosen division is that comparison values below 5 N/kPa are considered small and comparison values above 7.5 N/kPa are considered large.

5.1.2.1 Swimmers with small comparison values

5 swimmers, males 1, 2, 4 and 5 and female 1, have comparison values below 5 N/kPa. The measurements and the least-square fit for these swimmers are shown in Figure 5.2.

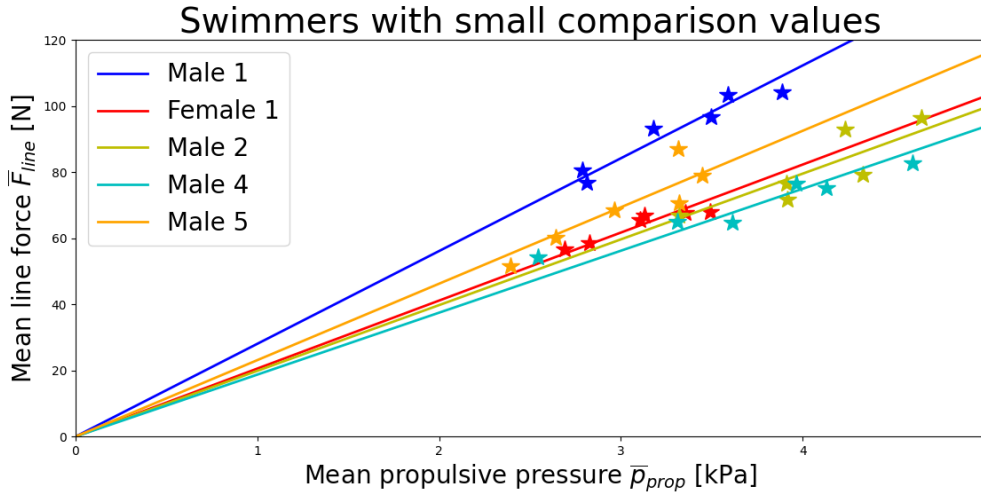


Figure 5.2: The figure shows the measurements on the 5 swimmers with small comparison values.

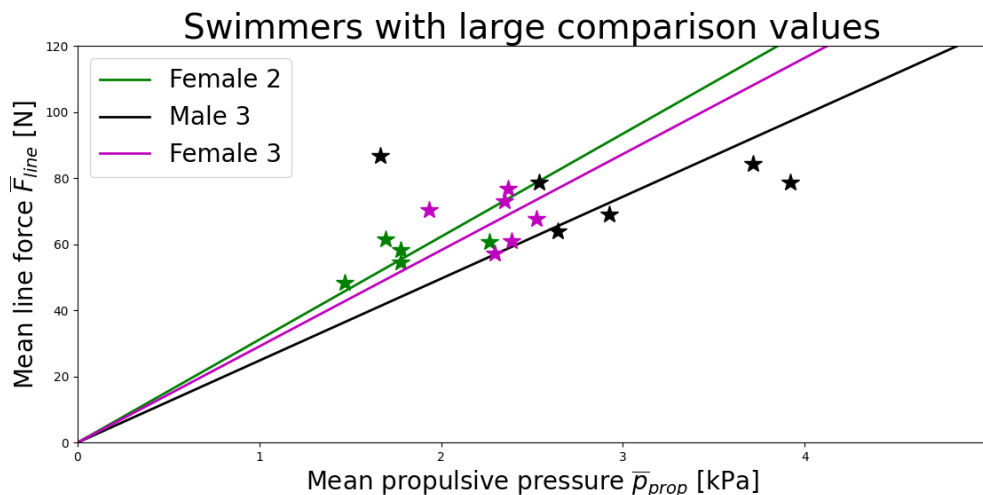
As indicated by the low comparison values, all measurements are close to the fitted line meaning that all measurements can be used when calculating A_e for each swimmer. These A_e values are shown in Table 5.2. It can be seen that all A_e values have a reasonable order of magnitude for being the area of a human arm.

Table 5.2: The table shows the calculated value of A_e for the swimmers with low comparison values.

Swimmer	A_e value [dm ²]
Male 1	2.808
Female 1	2.058
Male 2	1.990
Male 4	1.875
Male 5	2.314

5.1.2.2 Swimmers with large comparison values

3 swimmers, male 3, and female 2 and 3, have comparison values above 7.5 N/kPa. The measurements and the least-square fit for these swimmers are shown in Figure 5.3 where the least-square fit is performed with all measurement points considered.

**Figure 5.3:** The figure shows the measurements on the 3 swimmers with large comparison values.

For female 2 and 3 the large comparison values are caused by small $\bar{p}_{prop,span}$ values and the RMSE values are not much larger than for the swimmers with small comparison values. It is also hard to find any clear outliers among the measurements. The reasonable choice for female 2 and 3 is to keep all points when calculating A_e , but the small mean pressure difference range makes the tests unreliable.

For male 3 there are four points to the lower right that appears to follow a proportional line, while the two points to the top left seem to differ a lot from this proportionality. Therefore, the two points to the upper left are considered as outliers while the other points are used for determining A_e . This results in the least-square fits shown in Figure 5.4. For male 3, the RMSE value decreases to 5.429 N, the $\bar{p}_{prop,span}$ value decreases to 1.279 kPa and the comparison value decreases to 4.243 N/kPa.

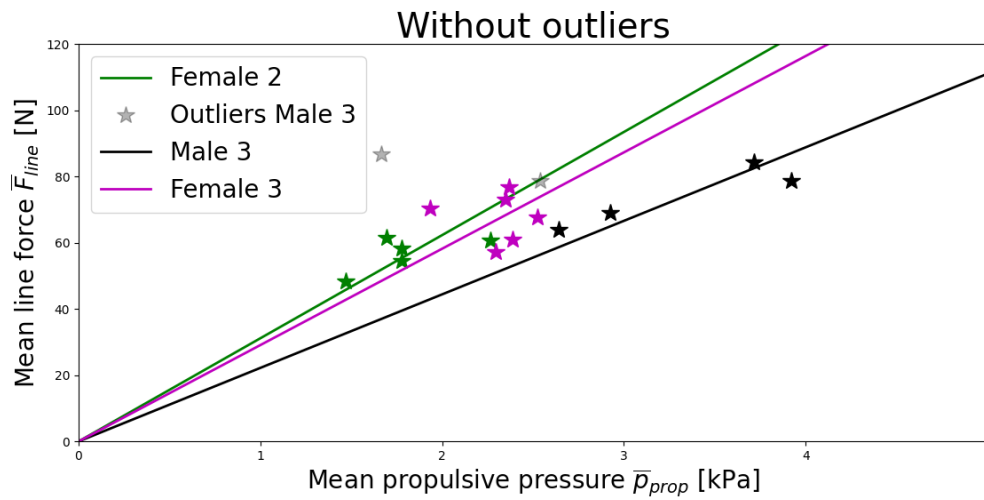


Figure 5.4: The figure shows the measurements on the 3 swimmers with large comparison values after the points determined as outliers have been removed.

The A_e values for these swimmers are shown in Table 5.3. It can be seen that all A_e values have a reasonable order of magnitude for being the area of a human arm.

Table 5.3: The table shows the determined value of A_e for the swimmers with larger comparison values after the determined outliers were removed.

Swimmer	A_e value [dm ²]
Female 2	3.117
Male 3	2.222
Female 3	2.911

6

Conclusion

6.1 Repeatability and accuracy

The repeatability part of this project indicates that the **eo** SwimBETTER handsets have a good repeatability regarding the mean cycle propulsive pressure $\bar{p}_{prop,c}$. This can be seen from the uncertainty in $\bar{p}_{prop,c}$ being close to the uncertainty in the cycle time t_{cycle} . It can also be seen that more uneven rotations (higher t_{cycle} uncertainties) can be related to higher $\bar{p}_{prop,c}$ uncertainties, which indicates that a part of the uncertainties found in this project can be attributed to uneven rotations.

It does not appear to be any difference between the left and right handset. Any differences noted in the measurements seem to be related to that the rig was not fully symmetric. Thereby, it is clear that the handset position on the hand can have an impact on the measurement, but it does not appear to be that big. This means that it should not be any problem as long as each individual swimmer mounts the handset similarly each time.

Some future improvements that were found for improving the repeatability measurements are as follows:

- The rig could be improved by using an electric motor instead of human power. This should make the rotations more identical and decrease the t_{cycle} uncertainty.
- The shaft of the rig could be made longer to extend the "arms" further out into the pool to decrease any effects of the pool wall.
- The rig being stationary means that each "stroke" is performed in turbulent water since the previous "strokes" have disturbed the water. This means that the water condition is not identical for each "stroke". This differs from normal swimming where the swimmer is constantly moving into non-turbulent water. One possibility would then be to build a new rig that can move along the side of a pool such that each "stroke" is performed in non-turbulent water.
- It could be possible to build a rig that can perform a stroke more similar to a normal swim stroke. This does, however, require more parts that can bend relative to each other meaning a more complicated rig and more coordination needed to ensure similar strokes.

For the sensor accuracy part, it is hard to draw any conclusions from the measurements performed. It should be noted that this part had the least focus in this project, and that the measurements could be improved easily if the raw pressure data from the handsets were available. If that would be the case, the measurements would be easier since it would be enough to lower the handsets to known depths

without any need to think about finding the maximum separation between the two pressure sensors. This would also enable comparisons against the true value and not just a comparison between two pressure sensors.

6.2 Force and power measurements

Of the nine swimmers studied, myself included, six showed promising results when it comes to the equivalent area hypothesis holding. Furthermore, two swimmers had results where the points were not separated enough to give any clear indication. This means that the idea of using force paddles and an equivalent area to measure the propulsive force seems promising. There is however a need for a larger study to get better results as well as some modifications that are needed for improving the method. These modifications are noted below:

- The swimmers should have more time to familiarize themselves with the hand-sets than the time that was available during this project.
- There is a need to ensure that the swimmers do not perform any flutter kick during the measurements. This was only said during the instructions, but it might be better to use an elastic band that physically hinders the swimmer from performing any flutter kick.
- As noted earlier, there were small separations between the points that were supposed to correspond to the different effort levels for some swimmers. It is also possible that individual swimmers interpret the effort levels differently. One solution for this could be to place some type of markers on the bottom of the pool and ask the swimmer to swim stationary at a certain marker instead of swimming at a certain effort level.
- One swimmer noted that it was hard to keep the legs floating even with the pull buoy. One option could be to mount another pull buoy between the ankles for more lift in the water.

6.2.1 Future work

When it comes to the force and power measurements in swimming, there are also some things that were not worked on at all during this project, but that are interesting to study in the future:

- Right now, it is only the propulsive force and not the power output that is measured. The next step is to determine how the full power measurement method should be performed.
- Once the power measurement method is determined, it would be interesting to compare the results from this method with the results from existing power measurement methods like VPM [4] and NABA [5].
- There is right now some manual work included in the calculations, for example exporting the propulsive pressure curves from the **eo** SwimBETTER webpage to the computer when calculating \bar{p}_{prop} , that could probably be automated to save time.
- So far the equivalent area of a swimmer is determined by experiments, meaning that time is needed for calibrating each swimmer before the propulsive force

and the power output can be measured. If the equivalent area instead could be calculated from measurements on the swimmers body (for example length, weight and arm length) it would simplify the conversion from pressure to force. This would however require that the equivalent area can be calculated from these body measurements without any large individual variations.

- A constant equivalent area is used so far, but it could be better to use an equivalent area that changes depending on the stroke phase. One option could be to use the depth of the hand to calculate how the instantaneous equivalent area should vary during the stroke.
- This project was focused of the arms since the **eo** SwimBETTER handsets are meant for measurements on the arms. It might however be possible to use a similar method with pressure sensors to measure the propulsive force from the legs. This option has been tried successfully for breaststroke kicking [31] and underwater kicking [32].
- So far, it is only freestyle that has been included in the measurements, but it could be possible to include other strokes. This might introduce some new difficulties, especially in butterfly, since performing fully tethered butterfly differs from normal butterfly more than fully tethered freestyle differs from normal freestyle.
- In longer swim races it is important to conserve the energy and get as much propulsive power as possible out of every breath of air. By combining propulsive power measurements with oxygen uptake measurements, for example in a flume (channel with flowing water), it should be possible to measure the efficiency of the swimmer by comparing the added power (the oxygen uptake) with the used power (propulsive power). This would enable more direct propulsive power measurements when calculating the swimming efficiency compared to indirectly using VPM like what is being done in [33].

Bibliography

- [1] Katherine Douglass et al. “Swimming in Data”. In: *The Mathematical Intelligencer* 46.2 (June 2024), pp. 145–155. DOI: 10.1007/s00283-024-10339-0.
- [2] eoLab. *SwimBETTER*. [Online; accessed 14-July-2024]. 2024. URL: <https://www.eolab.com/swimbetter>.
- [3] A. P. Hollander et al. “Measurement of active drag during crawl arm stroke swimming”. In: *Journal of Sports Sciences* 4.1 (1986), pp. 21–30. DOI: 10.1080/02640418608732094.
- [4] S.V. Kolmogorov and O.A. Duplishcheva. “Active drag, useful mechanical power output and hydrodynamic force coefficient in different swimming strokes at maximal velocity”. In: *Journal of Biomechanics* 25.3 (1992), pp. 311–318. ISSN: 0021-9290. DOI: 10.1016/0021-9290(92)90028-Y.
- [5] Angus Webb et al. “Prediction of passive and active drag in swimming”. In: *Procedia Engineering* 13 (2011). 5th Asia-Pacific Congress on Sports Technology (APCST), pp. 133–140. ISSN: 1877-7058. DOI: 10.1016/j.proeng.2011.05.063.
- [6] LOOK. *Power Pedals*. [Online; accessed 14-July-2024]. 2024. URL: <https://www.lookcycle.com/se-en/power-meter>.
- [7] Skisens AB. *Skisens: The future of skiing*. [Online; accessed 14-July-2024]. 2024. URL: <https://skisens.se/en/>.
- [8] One Giant Leap Ltd. *Paddle Smarter With Power*. [Online; accessed 14-July-2024]. 2023. URL: <https://onegiantleap.co.nz/>.
- [9] H.M. Toussaint et al. “Biomechanics of swimming”. In: *Exercise and sport science* (Jan. 2000), pp. 639–660.
- [10] Wikipedia. *Cycling power meter — Wikipedia, The Free Encyclopedia*. [Online; accessed 30-May-2024]. 2024. URL: https://en.wikipedia.org/wiki/Cycling_power_meter.
- [11] Roberto Cejuela, Héctor Arévalo-Chico, and Sergio Sellés-Pérez. “Power profile during cycling in World Triathlon series and olympic games”. In: *Journal of Sports Science & Medicine* 23.1 (2024), p. 25. DOI: 10.52082/jssm.2024.25.
- [12] Víctor Rodríguez-Rielves et al. “Torque-Cadence Profile and Maximal Dynamic Force in Cyclists: A Novel Approach”. In: *Sensors* 24.6 (2024). DOI: 10.3390/s24061997.
- [13] Cristian Romagnoli et al. “Paddle propulsive force and power balance: a new approach to performance assessment in flatwater kayaking”. In: *Sports Biomechanics* (2022), pp. 1–14. DOI: 10.1080/14763141.2022.2109505.

- [14] Paul William Macdermid and Philip W Fink. “The Validation of a Paddle Power Meter for Slalom Kayaking”. en. In: *Sports Med Int Open* 1.2 (Mar. 2017), E50–E57. DOI: 10.1055/s-0043-100380.
- [15] Pedro G Morouço et al. “Relative Contribution of Arms and Legs in 30 s Fully Tethered Front Crawl Swimming”. In: *BioMed Research International* 2015 (Oct. 2015), p. 563206. DOI: 10.1155/2015/563206.
- [16] Takaaki Tsunokawa et al. “The effect of using paddles on hand propulsive forces and Froude efficiency in arm-stroke-only front-crawl swimming at various velocities”. In: *Human Movement Science* 64 (2019), pp. 378–388. DOI: 10.1016/j.humov.2019.03.007.
- [17] Hideki Takagi and Barry Wilson. “Calculating hydrodynamic force by using pressure differences in swimming”. In: *Biomechanics and Medicine in Swimming* 8 (1999), pp. 101–106.
- [18] Swimming technology research. *Aquanex*. [Online; accessed 14-July-2024]. 2024. URL: <https://swimmingtechnology.com/aquanexanalysis/>.
- [19] Tomoya Kadi et al. “Novel Method for Estimating Propulsive Force Generated by Swimmers’ Hands Using Inertial Measurement Units and Pressure Sensors”. In: *Sensors* 22 (Sept. 2022), p. 6695. DOI: 10.3390/s22176695.
- [20] Daniel A. Marinho et al. “Smartpaddle® as a New Tool for Monitoring Swimmers’ Kinematic and Kinetic Variables in Real Time”. In: *The Open Sports Sciences Journal* 15 (Sept. 2022). DOI: 10.2174/1875399X-v15-e221026-2022-11.
- [21] Antti Löppönen et al. “The Effect of Paddle Stroke Variables Measured by Trainesense SmartPaddle® on the Velocity of the Kayak”. In: *Sensors* 22.3 (2022). DOI: 10.3390/s22030938.
- [22] Wikipedia. *Accuracy and precision* — *Wikipedia, The Free Encyclopedia*. [Online; accessed 12-May-2024]. 2024. URL: https://en.wikipedia.org/wiki/Accuracy_and_precision.
- [23] Prof. Motomu Nakashima. *Welcome to the website of Swimming Human Simulation Model "SWUM"!* [Online; accessed 14-July-2024]. 2023. URL: <http://www.swum.org/>.
- [24] Google. *Metronome*. [Online; accessed 14-July-2024]. 2024. URL: <https://g.co/kgs/Qk23nDQ>.
- [25] Dr Neil Baker, Assoc Prof Peter Sinclair, and Dr Kenneth Graham. *Static Pressure Testing of the Pressure Sensors on eo SwimBETTER PILOT*. [Online; accessed 14-July-2024]. 2023. URL: https://www.eolab.com/content/files/2023/06/08/eo_SwimBETTER_Pressure_Sensor_Evaluation.pdf.
- [26] Wikipedia. *Hydrostatics* — *Wikipedia, The Free Encyclopedia*. [Online; accessed 11-May-2024]. 2024. URL: <https://en.wikipedia.org/wiki/Hydrostatics>.
- [27] Wikipedia. *Newton’s laws of motion* — *Wikipedia, The Free Encyclopedia*. [Online; accessed 26-May-2024]. 2024. URL: https://en.wikipedia.org/wiki/Newton%27s_laws_of_motion.
- [28] NZ Manufacturing. *Long Belt Slider S11875-StrechCordz®*. [Online; accessed 14-July-2024]. 2020. URL: <https://nzcordz.com/product/strechcordz-long-belt-slider-3/>.

- [29] Wikipedia. *Root mean square deviation* — *Wikipedia, The Free Encyclopedia*. [Online; accessed 04-June-2024]. 2024. URL: https://en.wikipedia.org/wiki/Root_mean_square_deviation.
- [30] World Aquatics. *Swimming points*. [Online; accessed 14-July-2024]. 2024. URL: <https://www.worldaquatics.com/swimming/points>.
- [31] Takaaki Tsunokawa, Motomu Nakashima, and Hideki Takagi. “Use of pressure distribution analysis to estimate fluid forces around a foot during breaststroke kicking”. In: *Sports Engineering* 18.3 (Sept. 2015), pp. 149–156. DOI: 10.1007/s12283-015-0174-6.
- [32] Daiki Koga et al. “Comparison of foot pressure distribution and foot kinematics in undulatory underwater swimming between performance levels”. In: *Sports Biomechanics* 0.0 (2024), pp. 1–17. DOI: 10.1080/14763141.2024.2341014.
- [33] Sergei Kolmogorov, Andrei Vorontsov, and João Paulo Vilas-Boas. “Metabolic Power, Active Drag, Mechanical and Propelling Efficiency of Elite Swimmers at 100 Meter Events in Different Competitive Swimming Techniques”. In: *Applied Sciences* 11.18 (2021). DOI: 10.3390/app11188511.

A

Instantaneous propulsive pressure

Since the repeatability rig used in this project is stationary, the water becomes turbulent. This means that the initial conditions for each "stroke" is different and it is then hard to draw any conclusions for the repeatability of p_{prop} . To get a better picture of the instantaneous repeatability there is probably a need to use a rig that can move into "new" non-turbulent water for each stroke, similar to regular swimming. The p_{prop} profiles of the pull phase (from t_1 to t_2 , see Chapter 3.1.2) are however shown here without any analysis. The profiles shown are for the 100 bpm round 1 (number labels 1-4) and 100 bpm round 2 (number labels 5-8) measurements. A normalized time scale where t_1 is set to 0 and t_2 is set to 1 for every "stroke" is used and the mean p_{prop} profile is also shown for each handset.

A. Instantaneous propulsive pressure

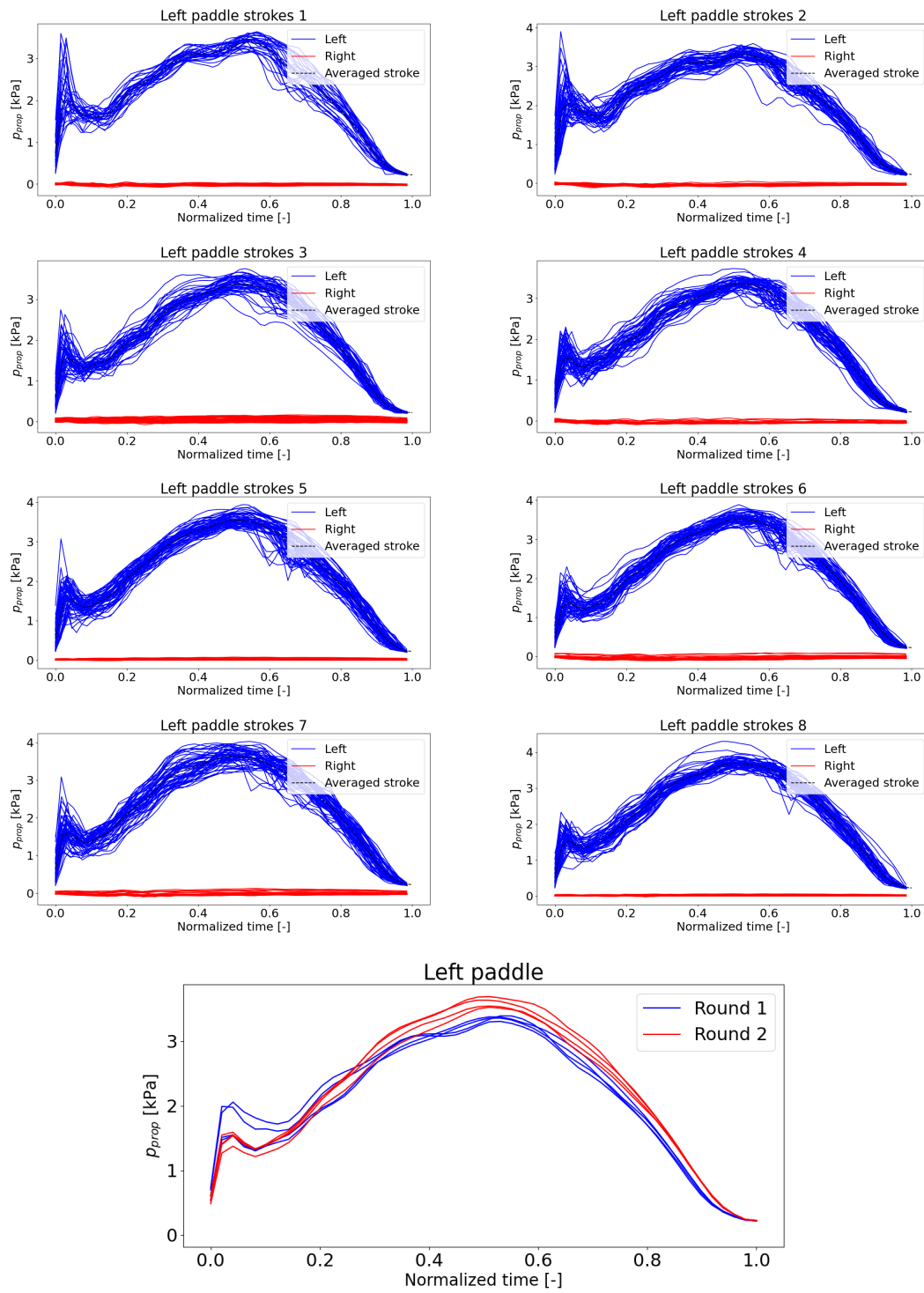


Figure A.1: The figure shows the p_{prop} profiles of the left handset "strokes".

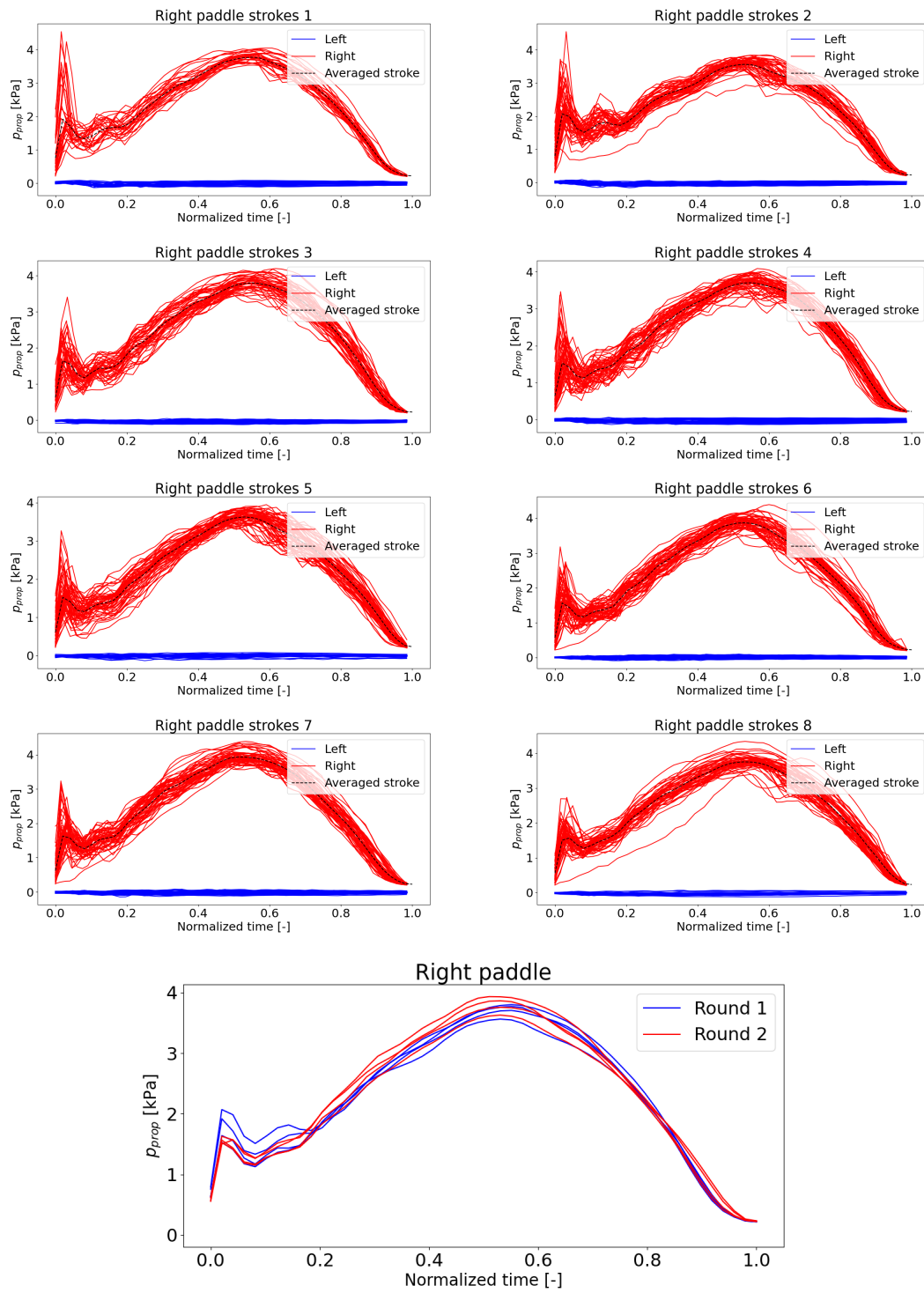


Figure A.2: The figure shows the p_{prop} profiles of the right handset "strokes".

DEPARTMENT OF INDUSTRIAL AND MATERIALS SCIENCE
CHALMERS UNIVERSITY OF TECHNOLOGY
Gothenburg, Sweden
www.chalmers.se



CHALMERS
UNIVERSITY OF TECHNOLOGY